

Spatial mapping of aquifer parameters over basaltic terrain of Maharashtra (India) using geophysical and hydro-geochemical information

G. Shailaja¹, G. Gupta*¹ and P. Rama Rao²

¹Indian Institute of Geomagnetism, New Panvel (W), Navi Mumbai 410218

²Department of Geophysics, Andhra University, Visakhapatnam 530 003

*Corresponding author: gupta_gautam1966@yahoo.co.in

ABSTRACT

Integrating the geoelectrical parameters with hydro-geochemical parameters of existing wells, the hydraulic conductivity, transmissivity and porosity of hard rock basaltic aquifers in a part of the semi-arid south-eastern region of Maharashtra were estimated. The hydraulic conductivity values were computed using the Kozeny–Carman–Bear (KCB) equation. The spatial variation of aquifer parameters was determined using the ordinary kriging technique. The results suggest that a number of isolated pockets of the study area reveal relatively high value of hydraulic conductivity, porosity and transmissivity. The hydraulic conductivity decreases with increasing bulk electrical resistivity due to possible presence of basaltic rock while, the increase of hydraulic conductivity with decrease of bulk electrical resistivity is presumably due to the good fracture network connectivity in crystalline hard rock. The transmissivity values at certain locations divulge high values (>380 m²/day), which are likely due to the water-saturated fractured medium. The derived transmissivity values are in good agreement with those obtained from well performance data of Central Ground Water Board (CGWB). These zones also have relatively high aquifer thickness and thus represent high potential regions within the water-bearing formations. The spatial variation map of transmissivity reveals a positive relationship with hydraulic conductivity at north-east, southern and western parts of the study area. These findings indicate that such studies would be useful in characterizing the aquifer system over different semi-arid, trap covered regions of India, including Maharashtra.

Key words: Vertical electrical sounding, hydro-geochemical parameters, hydraulic conductivity, kriging technique, transmissivity, porosity, Deccan Volcanic Province.

INTRODUCTION

Groundwater exploitation for domestic, agriculture and industrial purposes has tremendously increased over the last few decades that led to a rapidly growing consciousness about groundwater management. A quantitative portrayal of aquifer properties plays a critical role to understand the various hydrogeological processes. Fundamental aquifer characterization parameters such as hydraulic conductivity, transmissivity, formation factor and porosity are essential for a proper modeling of groundwater flow. Thus, spatial distribution of these parameters is vital in formulating strategies to manage the hydrological system. These types of studies are very significant in several hard rock terrains globally and particularly in Maharashtra, India, where the availability of surface and groundwater is meager due to erratic monsoon and unfavourable hydrological conditions.

Conventional procedure of calculating hydraulic conductivity from pumping tests at borehole sites is the most effective way, however drilling the wells at every vertical electrical sounding (VES) site to cover all the hydrogeological variations is not economical and also time consuming. Therefore, the aquifer parameters estimated

from the existing boreholes and resistivity parameters derived from surface resistivity measurements can be highly effective for the estimation of a host of hydraulic parameters such as, hydraulic conductivity, aquifer thickness, formation factor, porosity, and transmissivity. This is possible since the hydraulic and electrical aquifer properties are related to the pore space structure, grain size, grain shape and subsurface heterogeneity (Kelly, 1977; Mazáč et al., 1985; Christensen and Sorensen, 1998; De Lima et al., 2005). Niwas and Singhal (1981) advocated that the geology and groundwater quality are related and remains fairly constant within an area and thus relationships between aquifer properties and geophysical parameters can be construed.

Direct Current (DC) resistivity technique is widely used to address a variety of environmental, geological and geotechnical problems (El-Qady et al., 2000, Mondal et al., 2011; Maiti et al., 2013). It detects the resistivity differences within the subsurface and hence effective in estimating aquifer parameters related to the pore structure and heterogeneity (Rubin, 2003). But, as the current flow and conduction into the earth (i.e. lithology, grain size, grain shape etc) are extremely variable, the evaluation of

Spatial mapping of aquifer parameters over basaltic terrain of Maharashtra (India) using geophysical and hydro-geochemical information

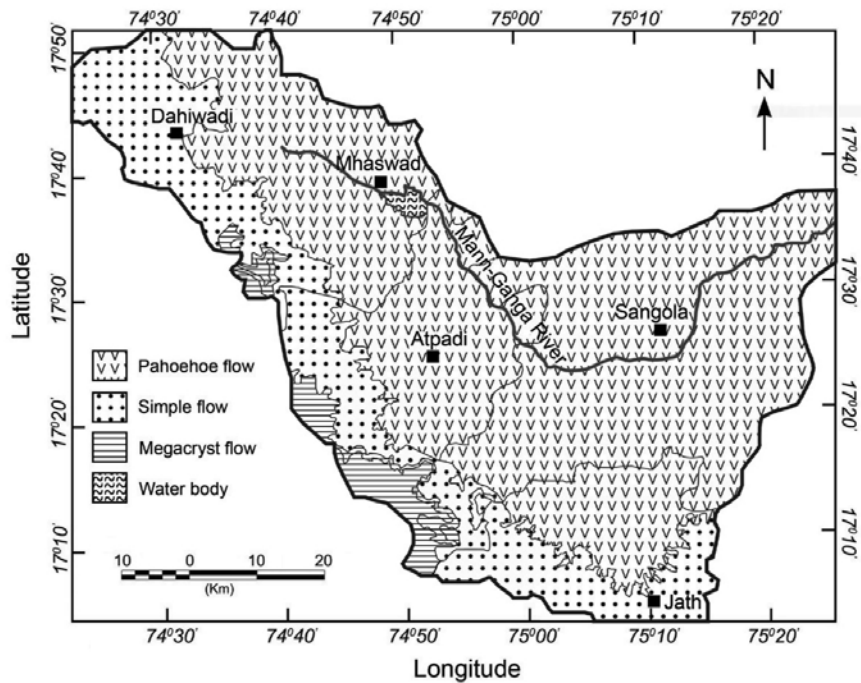


Figure 1. Geological map of the study area (after CGWB, 2013).

aquifer parameters (e.g. porosity, permeability) and their spatial variation is a challenging task (Das et al., 2016).

Many attempts have been made to construct statistical correlations between hydraulic conductivity and aquifer resistivity, for aquifer characterization as well as uncertainty estimation, particularly when borehole or geophysical data are sparse or unavailable. Also different data driven interpolation schemes have been developed to generate accurate and representative aquifer property maps (Webster and Oliver, 2001; Koehler and Peters, 2013; Das et al., 2016). Such schemes enable us to estimate the missing data between the sites with known data. In the present study, ordinary kriging interpolation technique is used to calculate the spatial variation of the aquifer parameters, as it gives better cross-validation results. Ordinary kriging is a geo-statistical method based on the linear conception of mapping that uses semi-variogram model fitting techniques to approximate values at unknown locations using the values at known locations (Webster and Oliver, 2001).

The primary aim of this study is to estimate the aquifer parameters and their spatial variability to give meaningful interpretation of aquifer properties and demonstrate its utility in the assessment and management of the groundwater resources of Mann River basin encompassing the districts of Satara, Solapur and Sangli located in the south-eastern part of Maharashtra, India. For this purpose, aquifer parameters such as hydraulic conductivity, formation factor, porosity and transmissivity are evaluated by utilizing electrical conductivity values

analyzed through hydro-geochemical analysis of existing dug wells and the respective vertical electrical sounding (VES) data in the study area.

Hydrogeology and Physiography of the Study Area

The study area falling under the Mann River basin extends from 17° 10' 00" to 17° 50' 00" of north latitudes and from 74° 20' 00" to 75° 30' 00" of east longitudes with a total area of 4753 sq. km. (Figure 1). The study area receives an average annual rainfall of about 500 mm, as it falls in the rain shadow region, which is a dry area on the lee side of the Western Ghats. Most of the places here are facing severe drought and several divisions have been classified as critical to semi-critical in ground water development. The western and north-western parts of the study area comprising hills and Ghats reveal very high elevation of 980 m above mean sea level a.m.s.l., while the north-eastern part covering foothill zones, plateaus and plains along the course of Mann River shows an altitude of 350 m a.m.s.l. The entire study area is predominantly covered by basaltic lava flows of late Cretaceous age. The area has undergone neo-tectonic activity as evidenced by varying fold, fault and lineaments (Tiware et al., 2001; Pandey et al., 2009).

Mann is the major river in the area and the drainage pattern is parallel to semi-dendritic with high drainage density. It rises near Mahadeo ranges near Phaltan in Satara district and flows to the west of Dahiwadi. It eventually turns towards Sangola and enters the Mangalweda sub-

division of Solapur district. The alluvial formation of recent age is thin and in isolated patches along the Mann River with limited areal extension (CGWB, 2013).

The groundwater occurs in the soil mantle and within the weathered/jointed/fractured basalts. The upper part of massive traps reveals persistent spheroidal weathering and exfoliation, which aids in retaining groundwater in these rocks in contrast to compact basalts (CGWB, 2013). The shallower zones down to depth of 20 m below ground level (bgl) form phreatic aquifer. The water bearing zones occurring between the depth of 20 m and 40 m are weathered interflow of shear zones and have water under semi-confined condition. Deep confined aquifers occur below the depth of 40 m (CGWB, 2013). However, the storage of groundwater in compact basalts depends on the presence of joints and their nature and inter-connectivity. It is reported that the average depth of dug wells in the region varies from 12-15 m bgl, while the bore wells reach up to about 60 m bgl. The yield of dug wells varies between 10 to 190 m³/day in cold season and between 5 to 20 m³/day in hot season (CGWB, 2013).

MATERIALS AND METHODS:

Conventionally, the aquifer hydraulic properties are obtained either from pumping tests or from laboratory core sample experiments (Soupios et al., 2007). In the present study, as bulk and water resistivities were obtained at several locations, hydraulic conductivity values were estimated using the Kozeny–Carman–Bear (KCB) equation (Domenico and Schwartz, 1990). The porosity (ϕ) required in KCB equation was calculated using Archie’s empirical law.

Archie’s empirical relation (Archie, 1942), relating bulk resistivity to porosity and fluid resistivity of a fully saturated granular medium is given by,

$$\rho_o = \alpha \rho_w \phi^{-m} \quad (1)$$

where ρ_o is the bulk resistivity, ρ_w is the fluid resistivity, ϕ is the porosity of the medium, m is known as the cementation factor, whose value increases with the compaction of the sediment, and the coefficient α is associated with the medium and its value is commonly assumed to be unity.

For a clay-free medium, the $\frac{\rho_o}{\rho_w}$ ratio is known as the intrinsic formation factor (F_i). Thus, Eq. (1) could be re-written in the following form,

$$\phi = e^{\frac{1}{m} \ln(\alpha) + \frac{1}{m} \ln\left(\frac{1}{F_i}\right)} \quad (2)$$

The values of the coefficients α and m should be determined for each site under investigation. However, as core samples were unavailable in the study area, an extensive range of values for α and m reported in published literature was used to obtain porosity values (Jackson et al., 1978; De Lima and Sharma, 1990).

In order to calculate the intrinsic formation factor in relation to the porosity of samples from different sites, Worthington (1993) described three different expressions. A fourth expression is advocated by Jackson et al., (1978) and De Lima and Sharma (1990), wherein the coefficient α is equal to 1 while m varies from 1.3 to 2.5. Nonetheless, a problem arises for actual field data due to the fact that Archie’s formula [Eqs. (1) and (2)] is applicable only for clay-free, clean, consolidated sediments. Any departure from these assumptions makes the equation invalid as argued by Worthington (1993). Thus, for unclean, clayey and shaley sands and a mixture of sand/gravels, some corrective steps for clay conductivity are required. In the present case, the coefficient α is equal to 1 while m is taken as 2.5. Several such models are currently in usage and majority of them are either shale-fraction or cation-exchange models which are essentially derived empirically using the concept of parallel conductor (Patnode and Wyllie, 1950; Winsauer and McCardell, 1953; Waxman and Smits, 1968; Sen et al., 1988).

The aquifer system in the present study area consists of clay, silt and sand material, and thus the Archie’s equation was modified, whereby the Waxman–Smits model was considered (Vinegar and Waxman, 1984) as it relates to the apparent formation factor (F_a) (which is the ratio of bulk resistivity to fluid resistivity) and intrinsic formation factor (F_i), after taking into account the shale effects. According to Worthington (1993),

$$\frac{1}{F_a} = \frac{1}{F_i} + \left(\frac{BQ_v}{F_i}\right) \rho_w \quad (3)$$

where the term BQ_v is related to the surface conduction, caused by clay particles. In case of no surface conduction effects, the apparent formation factor becomes equal to the intrinsic one.

A linear relation can be obtained between $1/F_a$ and ρ_w by re-arranging the terms of Eq. (3) as,

$$\frac{1}{F_a} = \frac{1}{F_i} + \left(\frac{BQ_v}{F_i}\right) \rho_w \quad (4)$$

where $1/F_i$ is the intercept of the straight line and BQ_v/F_i corresponds to the gradient (Worthington, 1993). Thus, by plotting $1/F_a$ with fluid resistivity ρ_w , one can obtain the value of intrinsic formation factor, to be subsequently used to estimate porosity using Eq. (2) as is shown in Table 1.

The above approach can be pursued by integrating the bulk resistivities (ρ_o) obtained from 1D resistivity inversion with the measured fluid electrical resistivities (ρ_w) obtained from the boreholes in the near vicinity of the VES locations. These values were then utilized to compute the apparent formation factor ($F_a = \rho_o/\rho_w$) of the aquifer. It is evident from Eq. (4) that a plausible cause of error would lead to the wrong estimation of the apparent formation factor, which depends on the bulk resistivity as estimated from the inversion models. Thus, if the fluid resistivities are measured in situ as accurately as possible and compared

Spatial mapping of aquifer parameters over basaltic terrain of
Maharashtra (India) using geophysical and hydro-geochemical information

Table 1: Estimation of formation factors and other aquifer parameters obtained from geophysical data

Water sample location	VES location	Fluid Resistivity (Ωm)	Bulk Resistivity (Ωm)	Aquifer thickness (m)	Fa	1/Fa	1/Fi	Porosity (%)	Hydraulic conductivity (m/day)	Transmissivity (m^2/day)
1	1	4.9652	1797	15.5	361.92	0.0028	0.0006	27.3	1.293	20.049
2	2	23.31	139	9.28	5.96	0.1677	0.0072	42.4	7.72	71.637
3	3	12.4533	1142	6.55	91.70	0.0109	0.0009	29.4	1.713	11.221
4	4	21.7391	149	21.3	6.85	0.1459	0.0067	41.9	7.322	155.958
5	5	6.4935	15.1	6.64	2.33	0.4300	0.0662	62.4	57.745	383.429
6	6	2.2188	84.8	0.553	38.22	0.0262	0.0118	46.2	11.447	6.33
7	7	3.3322	94.3	20.4	28.30	0.0353	0.0106	45.4	10.547	215.155
8	8	3.4282	169	20.7	49.30	0.0203	0.0059	41.0	6.653	137.707
9	9	18.8679	1569	8.85	83.16	0.0120	0.0006	27.8	1.385	12.256
10	10	7.9554	176	14.6	22.12	0.0452	0.0057	40.7	6.442	94.052
11	11	11.4155	36.2	8.33	3.17	0.3153	0.0276	53.6	24.032	200.19
12	12	26.0417	73.8	55.9	2.83	0.3529	0.0136	47.4	12.933	722.961
13	13	5.184	146	15.6	28.16	0.0355	0.0068	42.1	7.479	116.668
14	14	8.3195	235	12.2	28.25	0.0354	0.0043	38.7	5.183	63.228
15	15	6.4309	106	25	16.48	0.0607	0.0094	44.5	9.612	240.311
16	16	7.9618	415	0.628	52.12	0.0192	0.0024	35.1	3.45	2.166
17	17	13.986	206	0.934	14.73	0.0679	0.0049	39.6	5.719	5.342
18	18	7.3421	814	4.44	110.87	0.0090	0.0012	31.2	2.156	9.572
19	19	7.6511	2271	29.8	296.82	0.0034	0.0004	26.2	1.11	33.063
20	20	7.3692	362	14.2	49.12	0.0204	0.0028	35.9	3.784	53.727
21	21	4.7483	22.5	10.8	4.74	0.2110	0.0444	58.2	37.91	409.43
22	22	4.0355	9385	1.85	2325.61	0.0004	0.0001	20.2	0.435	0.805
23	23	10.1729	33.1	4.75	3.25	0.3073	0.0302	54.4	26.014	123.566
24	24	2.6302	309	3.86	117.48	0.0085	0.0032	36.9	4.24	16.366
25	25	2.8121	39.8	8.11	14.15	0.0707	0.0251	52.7	21.981	178.266
26	26	15.9744	1036	64.7	64.85	0.0154	0.0010	29.9	1.828	118.255
27	27	17.762	204	6.69	11.49	0.0871	0.0049	39.7	5.782	38.681
28	28	4.029	1338	75.7	332.09	0.0030	0.0007	28.6	1.542	116.718
29	29	8.1169	269	5.96	33.14	0.0302	0.0037	37.8	4.691	27.956
30	30	10.5708	38.6	5	3.65	0.2739	0.0259	53.0	22.645	113.225
31	31	1.1811	869	28.5	735.75	0.0014	0.0012	31.0	2.102	59.92
32	32	17.331	23.6	2.38	1.36	0.7344	0.0424	57.7	36.073	85.854
33	33	3.349	31.7	4.69	9.47	0.1056	0.0315	54.9	27.334	128.196
34	34	8.5911	2896	0.507	337.09	0.0030	0.0003	25.1	0.947	0.48
35	35	8.3056	37.3	6.21	4.49	0.2227	0.0268	53.3	23.329	144.87
36	36	6.6269	1589	14.6	239.78	0.0042	0.0006	27.8	1.385	20.219
37	37	5.0251	912	6.86	181.49	0.0055	0.0011	30.6	1.999	13.712
38	38	15.0602	381	12.9	25.30	0.0395	0.0026	35.6	3.655	47.153
39	39	19.1571	372	51.1	19.42	0.0515	0.0027	35.8	3.74	191.135
40	40	13.2275	346	12.1	26.16	0.0382	0.0029	36.2	3.916	47.382
41	41	5.872	5206	4.48	886.58	0.0011	0.0002	22.5	0.637	2.855

to available resistivity and litholog information from close by boreholes, the error can then be quantified by the variation of inverted resistivity values. However, this approach may introduce some ambiguity due to the fact that some of the borehole locations were at distance away from the VES sites.

Table 1 gives the resistivity and thickness values obtained from the inversions and the calculated apparent formation factors. By applying least square best fit linear approach of the individual groups of the data between $1/F_a$ and fluid resistivity (ρ_w), the range of the inverse of intrinsic formation factor F_i is calculated. In the present case, F_i varies from 1.3617 to 5525.374 as shown in Table 1. The porosities can now be calculated using Eq. 2 for the reported values of α and m (Table 1).

The hydraulic conductivity (k) was determined using the KCB equation (Domenico and Schwartz, 1990) as,

$$k = \left(\frac{\delta_w g}{\mu} \right) \cdot \left(\frac{d^2}{180} \right) \cdot \left[\frac{\phi^3}{(1-\phi^2)} \right] \quad (5)$$

where, d is the grain size (0.01 cm), δ_w is the fluid density (taken to be 1000 kg/m³), and μ is the dynamic viscosity (taken to be 0.0014 kg/ms) (Fetter, 1994). The estimated hydraulic conductivity values using Eq. (5) are provided in Table 1.

In the present study, the spatial variability of aquifer parameters were determined using the ordinary kriging technique, which is a linear stochastic method using semi-variogram model fitting schemes in order to evaluate values at unknown sites using the values at known sites (Webster and Oliver, 2001; Das et al., 2016).

Correlation of hydraulic parameters

The correlation plot is obtained between fluid resistivity (ρ_w) and inverted formation factor ($1/F_a$) to calculate the intrinsic formation factor (F_i) Figure 2a, revealing a straight line with slope 0.0222 and intercept value of -0.1132 and giving the coefficient of determination of 0.8506. A positive linear relation between fluid resistivity (ρ_w) and inverted formation factor is obtained as shown in Figure 2a having equation

$$\frac{1}{F_a} = 0.0222\rho_w + (-0.1132) \quad (6)$$

This suggests that as the fluid resistivity increases, the formation factor gradually decreases, which satisfies the Archie's equation for finding formation factor i.e. the ratio of bulk resistivity to fluid resistivity.

The correlation plot obtained between bulk resistivity and hydraulic conductivity is shown in Figure 2b. A negative relation between these two parameters is observed suggesting that the hydraulic conductivity decreases with increasing bulk electrical resistivity due to possible presence of basaltic rock and granitic gneiss (Das et al., 2016). In contrast, the increase of hydraulic conductivity

with decrease of bulk electrical resistivity could be due to the superior connectivity of fracture network in crystalline hard rock. This result is in agreement with the response curve obtained between bulk resistivity and hydraulic conductivity over un-weathered hard rock terrain (Singh, 2005). The exponential fit is satisfactory to derive a nonlinear relationship between bulk resistivity and hydraulic conductivity such that,

$$k = -0.0005e^{2.078\rho_b} \quad (7)$$

The least square fit between two parameters gives coefficient of determination value of 0.4629, slope of -0.0005 and intercept 2.078.

RESULTS AND DISCUSSION:

Spatial variability of aquifer thickness

The aquifer thickness contour map Figure 3 produced using ordinary kriging procedure reveals higher aquifer thickness in the central western part with thickness ranging from 25–70 m. This zone is surrounded by the foothills of Western Ghats and prominent town of Atpadi Figure 3. Similarly, thick aquifer zones are revealed in small stretches of north-eastern and central eastern part Figure 3. Here the thickness varies from 30-60 m. This variation in aquifer thickness can be attributed to topography and varied composition and structure of favourable and unfavourable subsurface layers of confined and semi-confined nature prevalent in this region. As mentioned earlier, the shallow groundwater zones develop down to depth of 20 m bgl while the water bearing zones at depth of 20 m and 40 m are found under semi-confined condition. In this region, deep confined aquifers occur below the depth of 40 m. The average depth of dug wells in the region fluctuates from 12-15 m bgl. Making use of thickness and depth extent of groundwater zones, the bore wells are in general drilled up to 60 m bgl. Figure 3 details about groundwater horizon depths, which could be used in future to approximately fix up the drilling depth in this region to penetrate the thick aquifer.

Spatial variability of porosity

The contour map for porosity constructed using ordinary kriging method Figure 4 reveals varying porosities over the entire study area. High values of the order of 45-60 % are predominant along the course of Mann River. This could be due to alluvial formation that is seen in isolated patches along the Mann River, which results in high porosity content. A small part in western and southern side also depicts high porosity. It is envisaged that the high value of porosity are indicative of zones of high potential within the water-bearing formation. The porosity variation map is mainly controlled by lithology, grain size of rock, packing of grain-size and various agricultural practices in this region.

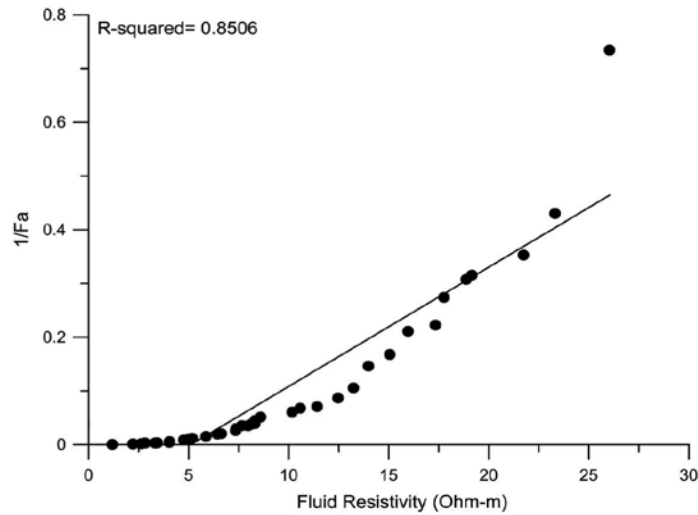


Figure 2a: Determination of the intrinsic formation factor F_1 by plotting $1/F_a$ versus fluid resistivity ρ_w .

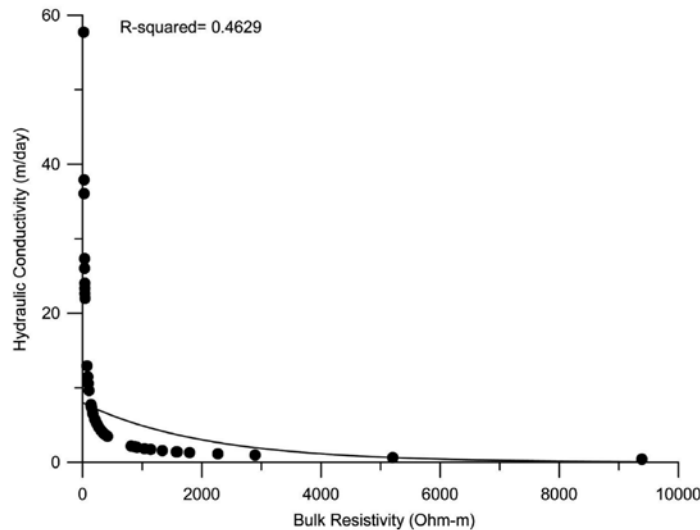


Figure 2b: Correlation plot between bulk resistivity and hydraulic conductivity (k).

It has been reported by Deolankar (1980) that the weathered basalt shows highest aggregate porosity (34 %) in Deccan Volcanic Province (DVP), whereas the specific yield is less (around 7 %). Though the porosity is high, the specific yield is very small indicative of higher specific retention of the weathered basalt. This may be caused due to the presence of clay minerals in the weathered basalt which has higher water retention capacity.

Spatial variability of Hydraulic conductivity

The hydraulic conductivity (k) has been estimated as discussed earlier and its contour map constructed using ordinary kriging procedure Figure 5. It suggests high values (>22 m/day) around Atpadi and east of Sangola. Hydraulic conductivity is also high in the vicinity of Jath (about 37 m/day) in the southern fringe of the study area coinciding

with high porosity values, wherein the grain size is very fine suggesting that the geological medium could be fractured. It is reported that in hard rock terrain, the rock matrix and fractures therein reveal different properties, which divulge that the flow pattern is influenced by the geometric properties of the fractures and the connectivity in fracture-network (Schwartz and Zhang, 2004; Das et al., 2016). Furthermore, fracture density and its direction is a crucial attribute contributing to the hydraulic conductivity of a fractured rock system (Schwartz and Zhang, 2004). It is well known that only interconnected fractures offer better conduit for groundwater flow and contaminant transport (Das et al., 2016). This means that fractures trending parallel to the hydraulic gradient are likely to provide efficacious pathways than fractures trending perpendicular to the hydraulic gradient. The enhancement of hydraulic conductivity with the decline of bulk resistivity is obvious

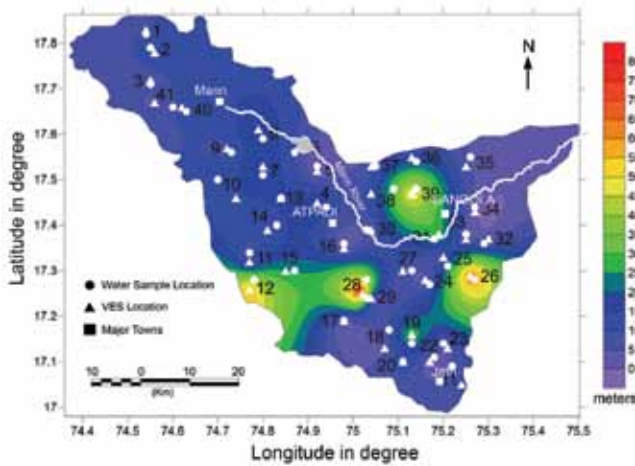


Figure 3: Spatial variability map of aquifer thickness. Locations of VES and bore wells are shown to have a comprehensive view.

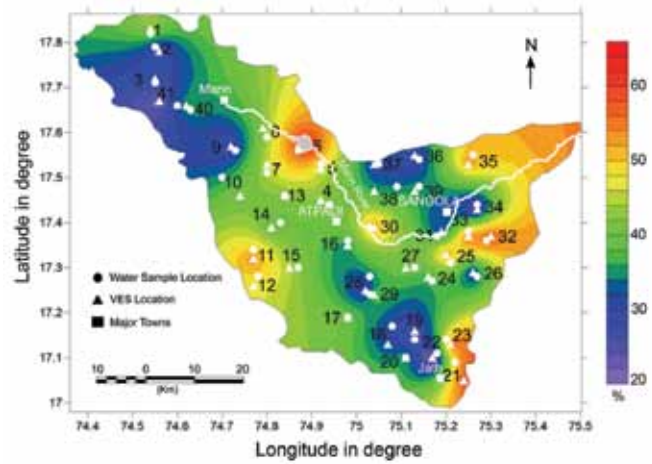


Figure 4: Spatial variability map of porosity. Locations of VES and bore wells are shown to have a comprehensive view.

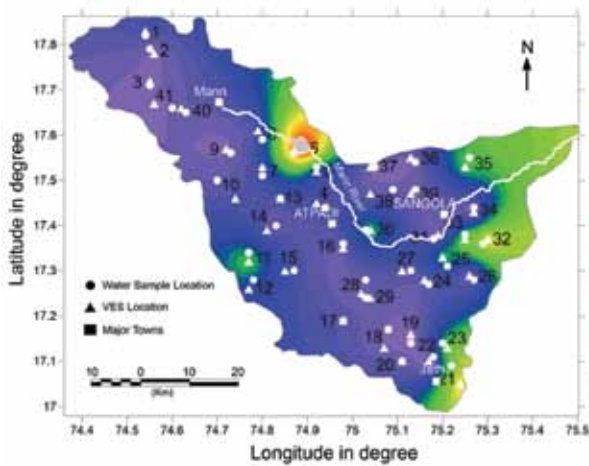


Figure 5: Spatial variability map of hydraulic conductivity. Locations of VES and bore wells are shown to have a comprehensive view.

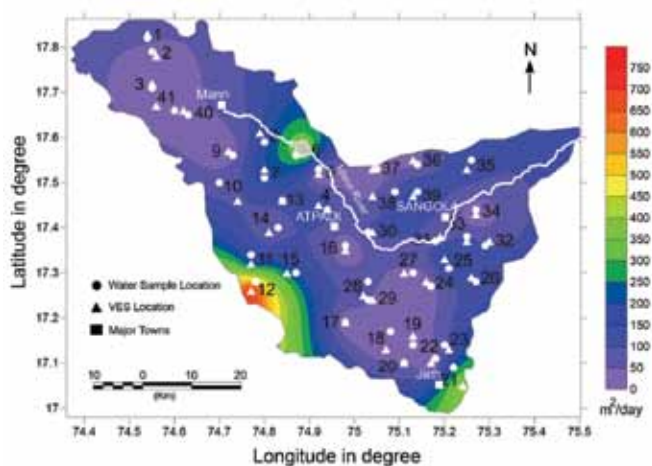


Figure 6: Spatial variability map of transmissivity. Locations of VES and bore wells are shown to have a comprehensive view.

in the area because the fractured medium could be saturated with water due to Mann River and its tributaries. It can be inferred that the spatial variability in hydraulic conductivity is largely controlled by porosity and fracture fabric in the study area.

Spatial variability of Transmissivity

Transmissivity (T) is the product of hydraulic conductivity (k) and aquifer thickness. The transmissivity in the study area has been calculated and its contour map was constructed using ordinary kriging procedure and is shown in Figure 6. It is observed that the T values vary from 0.48-723 m^2/day . High T values (723, 409 and 383 m^2/day) is observed in the northern, southern and western

parts of the study area, respectively. High values are likely due to the fractured medium, saturated with water. This in turn represents high potential within the water-bearing formation. It may be recollected from previous sections that the aquifer thickness is relatively high over these areas (10-65 m), and transmissivity is directly proportional to aquifer thickness. Therefore these areas divulge high transmissivity values. Also the fracture matrix might be well connected at deeper depths, thereby giving rise to good inter-fracture connectivity.

The present findings fairly corroborate with the T values of 30-450 m^2/day in and around Mann, west of Atpadi and Jath, obtained by CGWB (2013). Transmissivity values (CGWB, 2013) in the eastern part, near Sangola, are of the order of 1.25-210 m^2/day , which are rather low.

From Figure 6 it can be seen that the T values in the eastern sector range from 0.48-191 m²/day, which are in fair agreement with the well data values of CGWB (2013).

The spatial variation map of transmissivity Figure 6 reveals a positive correlation with hydraulic conductivity at north-east, southern and western parts. However, at eastern part, there is a mismatch between the transmissivity and hydraulic conductivity. Though the hydraulic conductivity is high, low transmissivity values are reflected as the aquifer thickness is too less. This suggests that this part of the study area may not sustain large production wells.

CONCLUSIONS

Details of aquifer parameters by using VES and geochemical attributes of Mann River basin located in the south-eastern part of Maharashtra are presented. The study can significantly contribute to the understanding of the aquifer characteristics in regions that lack pumping test data. The relation between bulk resistivity and hydraulic conductivity is established, wherein a negative correlation is obtained between the two parameters, i.e., the hydraulic conductivity of the aquifer is exponentially decreasing with increasing bulk resistivity. Further, spatial variation maps of aquifer parameters like transmissivity, hydraulic conductivity, aquifer thickness and porosity were computed and contoured using ordinary kriging technique.

The estimated transmissivity of the geological formations in the study area shows a wide range varying between 0.48 and 723 m²/day, due to the high structural and compositional inhomogeneity of the basaltic formations. The high values of transmissivity could be due to the presence of fractured medium saturated with water, suggesting high potential within the water-bearing formation. The T values revealed here are in good agreement with the values obtained from pumping test data of CGWB (2013). The calculated hydraulic conductivity parameter reveals high values (>22 m/day) near the central part of the basin, east of Sangola and near Jath in the south-eastern part of the study area. This is due to high porosity values because the grain size is very fine. The high porosity also advocates that the geological medium could be fractured and indicative of high potential water-bearing formations.

It can be concluded from the present study that geoelectrical sounding technique can be effectively used not only for groundwater investigation but also for integrating it with hydro geochemical parameters for estimating the hydraulic parameters of the aquifer. This scheme is cost effective and can significantly reduce the amount of test drilling. The tested integrated approach can be relied upon to provide rapid complementary data for the evaluation of groundwater potential, especially in hard-rock terrain of the country.

ACKNOWLEDGEMENTS

The authors are obliged to Dr. D.S. Ramesh, Director, IIG, Mumbai for the support and according permission to publish this work. The authors are indebted to Dr. M.R.K. Prabhakara Rao and Prof.B.Venkateswara Rao for in depth reviewing of the manuscript and useful suggestions to improve quality of the manuscript. Thanks are due to Shri B.I. Panchal for drafting the figures. The authors are grateful to Dr.P.R.Reddy, Chief Editor for continued support, constructive suggestions and final editing.

Compliance with Ethical Standards:

The authors declare that they have no conflict of interest and adhere to copyright norms.

REFERENCES

- Archie, G.E., 1942. The electrical resistivity log as an aid in determining some reservoir characteristics, American Institute of Mineral and Metal Engineering, Technical Publication 1422, Petroleum Technology, pp: 8-13.
- CGWB, 2013. Groundwater information, Sindhudurg district, Maharashtra, Technical Report, 1798, 1803, 1805, / DBR/2013, Central Ground Water Board, Ministry of Water Resources.
- Christensen, N.B., and Sorensen, K.I., 1998. Surface and borehole electric and electromagnetic methods for hydrogeological investigations, European Jour. Environ. Engg. Geophys., v.31, pp: 75-90.
- Das, A., Maiti, S., Suneetha, N., and Gupta, G., 2016. Estimation of spatial variability of aquifer parameters from geophysical methods: A case study of Sindhudurg district, Maharashtra, India, Stoch. Environ. Res. Risk Assess, DOI: 10.1007/s00477-016-1317-4.
- De Lima, O.A.L., Clennell, M.B., Nery, G.G., and Niwas, S., 2005. A volumetric approach for the resistivity response of freshwater shaly sandstones, Geophysics, v.70, no.1, pp: 1-10.
- De Lima, O.A.L., and Sharma, M.M., 1990. A grain conductivity approach to shaly sand, Geophysics, v.50, pp: 1347-1356.
- Deolankar, S.B., 1980. The Deccan Basalt of Maharashtra, India-their potential as aquifers, Groundwater, v.18, no. 5, pp. 434-437.
- Domenico, P.A., and Schwartz, F.W., 1990. Physical and Chemical Hydrogeology, Wiley, New York, pp: 324.
- El-Qady, G., Ushijima, K. and El-Sayed, A., 2000. Delineation of a geothermal reservoir by 2D inversion of resistivity data at Hammam Faraun area, Sinai, Egypt, Proceeding World Geothermal Congress, pp: 1103-1108.
- Fetter, C.W., 1994. Applied Hydrogeology, 3rd edn., Prentice-Hall, Inc., New Jersey, p: 600

- Jackson, P.D., Taylor-Smith, D. and Stanford, P.N., 1978. Resistivity-porosity-particles shape relationships for marine sands, *Geophysics*, v.43, pp: 1250-1268.
- Kelly, W., 1977. Geoelectric sounding for estimating aquifer hydraulic conductivity, *Groundwater*, v.15, no.6, pp: 420-425.
- Koehler, K.A., and Peters, T., 2013. Influence of analysis methods on interpretation of hazard maps, *Ann. Occup. Hyg.*, v.57, no.5, pp: 558-570.
- Maiti, S., Gupta, G., Erram, V.C., and Tiwari, R.K., 2013. Delineation of shallow resistivity structure around Malvan, Konkan region, Maharashtra by neural network inversion using vertical electrical sounding measurements, *Environ. Earth Sci.*, v.68, pp: 779-794.
- Mazáč, O., Kelly, W.E., and Landa, I., 1985. A hydrogeophysical model for relations between electrical and hydraulic properties of aquifers, *J. Hydrol.*, v.79, no.1-2, pp: 1-19.
- Mondal, N.C., Singh, V.S., Saxena, V.K., and Singh, V.P., 2011. Assessment of seawater impact using major hydrochemical ions: a case study from Sadras, Tamilnadu, India, *Environ. Monit. Assess.*, v.177, pp: 315-335.
- Niwas, S., and Singhal, D.C., 1981. Estimation of aquifer transmissivity from Dar-Zarrouk parameters in porous media, *J. Hydrol.*, v.50, pp: 393-399.
- Pandey, O.P., Chandrakala, K., Parthasarathy, G., and Reddy, P.R., 2009. Upwarped high velocity mafic crust, subsurface tectonics and causes of intraplate Latur-Killari (M 6.2) and Koyna (M 6.3) earthquakes, India- A comparative study, *J. Asian Earth Sci.*, v.34, pp: 781-795.
- Patnode, W.H., and Wyllie, M.R.J., 1950. The presence of conductive solids in reservoir rocks as factor in electric log interpretation, *Pet. Trans. Am. Inst. Min. Metall. Pet. Engg.*, v. 189, pp: 47-52.
- Rubin, Y., 2003. *Applied stochastic hydrogeology*. Oxford Univ. Press, New York, 416 p.
- Schwartz, W.F., and Zhang, H., 2004. *Fundamentals of groundwater*, Wiley, New York, p 583.
- Sen, P.N., Goode, P.A., and Sibbit, A., 1988. Electrical conduction in clay bearing sandstones at low and high salinities, *J. Appl. Phys.*, v.63, pp: 4832-4840.
- Singh, K.P., 2005. Nonlinear estimation of aquifer parameters from surficial resistivity measurements, *Hydrol. Earth Syst. Sci. Discuss.*, v.2, pp: 917-938.
- Soupios, P.M., Kouli, M., Vallianatos, F., Vafidis, A., and Stavroulakis, G., 2007. Estimation of aquifer hydraulic parameters from surficial geophysical methods: a case study of Keritis Basin in Chania (Crete-Greece), *J. Hydrol.*, v.338, pp: 122-131.
- Tiwari, V.M., Vyaghreswara Rao, M.B.S., and Mishra, D.C., 2001. Density inhomogenities beneath Deccan Volcanic Province, India as derived from gravity data, *J. Geodynamics*, v.31, pp: 1-17.
- Vinegar, H.J., and Waxman, M.H., 1984. Induced polarisation of shaly sands, *Geophysics*, v.49, no. 8, pp: 1267-1287.
- Waxman, M.H., and Smits, L.J.M., 1968. Electrical conductivities in oil bearing sands, *J. Soc. Pet. Engg.*, v.8, pp: 107-122.
- Webster, R. and Oliver, M.A., 2001. *Geostatics for environmental scientists*, Wiley, Chichester.
- Winsauer, W.O., and McCardell, W.M., 1953. Ionic double-layer conductivity in reservoir rock, *Trans. Am. Inst. Min. Metall. Pet. Eng.*, v.198, pp: 129-134.
- Worthington, P.F., 1993. The uses and abuses of the Archie's equation: the formation factor - porosity relationship, *J. Appl. Geophys.*, v.30, pp: 215-228.

Received on 15.8.17; Revised on: 28.9.17; Accepted on: 2.10.17